



THE UNIVERSITY *of* EDINBURGH

## Edinburgh Research Explorer

### Risks to carbon storage from land-use change revealed by peat thickness maps of Peru

**Citation for published version:**

Hastie, A, Honorio Coronado, EN, Reyna, J, Mitchard, E, Åkesson, CM, Baker, TR, Cole, LES, Córdova Oroche, CJ, Dargie, G, Dávila, N, De Grandi, E, Del Aguila, J, Del Castillo Torres, D, Cruz Paiva, RDL, Draper, FC, Flores, G, Grández, J, Hergoualc'h, K, Householder, JE, Janovec, JP, Lähteenoja, O, Reyna, D, Rodríguez-Veiga, P, Roucoux, KH, Tobler, M, Wheeler, C, Williams, M & Lawson, IT 2022, 'Risks to carbon storage from land-use change revealed by peat thickness maps of Peru', *Nature Geoscience*, vol. 15, pp. 369–374. <https://doi.org/10.1038/s41561-022-00923-4>

**Digital Object Identifier (DOI):**

[10.1038/s41561-022-00923-4](https://doi.org/10.1038/s41561-022-00923-4)

**Link:**

[Link to publication record in Edinburgh Research Explorer](#)

**Document Version:**

Peer reviewed version

**Published In:**

Nature Geoscience

**General rights**

Copyright for the publications made accessible via the Edinburgh Research Explorer is retained by the author(s) and / or other copyright owners and it is a condition of accessing these publications that users recognise and abide by the legal requirements associated with these rights.

**Take down policy**

The University of Edinburgh has made every reasonable effort to ensure that Edinburgh Research Explorer content complies with UK legislation. If you believe that the public display of this file breaches copyright please contact [openaccess@ed.ac.uk](mailto:openaccess@ed.ac.uk) providing details, and we will remove access to the work immediately and investigate your claim.



# Risks to carbon storage from land-use change revealed by peat thickness maps of Peru

Adam Hastie<sup>1</sup>, Eurídice N. Honorio Coronado<sup>2,3</sup>, José Reyna<sup>3</sup>, Edward T. A. Mitchard<sup>1</sup>, Christine M. Åkesson<sup>2</sup>, Timothy R. Baker<sup>4</sup>, Lydia E. S. Cole<sup>2</sup>, César. J. Córdova Oroche<sup>3</sup>, Greta Dargie<sup>4</sup>, Nállarett Dávila<sup>3</sup>, Elsa Carla De Grandi<sup>1</sup>, Jhon Del Águila<sup>3</sup>, Dennis Del Castillo Torres<sup>3</sup>, Ricardo de la Cruz Paiva<sup>5</sup>, Frederick C. Draper<sup>4,6</sup>, Gerardo Flores<sup>3</sup>, Julio Grández<sup>3</sup>, Kristell Hergoualc'h<sup>7</sup>, J. Ethan Householder<sup>8</sup>, John P. Janovec<sup>9</sup>, Outi Lähteenoja<sup>10</sup>, David Reyna<sup>3</sup>, Pedro Rodríguez-Veiga<sup>11,12</sup>, Katherine H. Roucoux<sup>2</sup>, Mathias Tobler<sup>13</sup>, Charlotte E. Wheeler<sup>1,7</sup>, Mathew Williams<sup>1,14</sup>, Ian T. Lawson<sup>2</sup>.

## Affiliations

- 1 School of GeoSciences, University of Edinburgh, Edinburgh, United Kingdom
- 2 School of Geography and Sustainable Development, University of St Andrews, St Andrews, United Kingdom
- 3 Instituto de Investigaciones de la Amazonía Peruana (IIAP), Av. Abelardo Quiñonez km 2.5, Iquitos, Perú
- 4 School of Geography, University of Leeds, Leeds, United Kingdom
- 5 Servicio Nacional Forestal y de Fauna Silvestre, Avenida Javier Prado Oeste, Magdalena del Mar, Lima, Perú
- 6 Center for Global Discovery and Conservation Science, Arizona State University, AZ, United States of America
- 7 Center for International Forestry Research (CIFOR), Jl. CIFOR, Situ Gede, Bogor, 16115, Indonesia
- 8 Wetland Ecology, Institute for Geography and Geoecology, Karlsruhe Institute for Technology, Karlsruhe, Germany
- 9 Sam Houston State University Natural History Museum, Sam Houston State University, Huntsville, TX, USA
- 10 Helsinki, Finland
- 11 Centre for Landscape and Climate Research (CLCR), School of Geography, Geology and Environment, University of Leicester, University Road, Leicester LE1 7RH, UK
- 12 National Centre for Earth Observation, University of Leicester, Space Park Leicester, Corporation Road, Leicester LE4 5SP, UK
- 13 San Diego Zoo Global, Institute for Conservation Research, 15600 San Pasqual Valley Road, Escondido, CA, USA
- 14 NCEO, University of Edinburgh, UK

## Abstract

Tropical peatlands are among the most carbon dense ecosystems but land-use change has led to the loss of large peatland areas, associated with substantial greenhouse gas emissions. In order to design effective conservation and restoration policies, maps of the location and carbon storage of tropical peatlands are vital. This is especially so in countries such as Peru where the distribution of its large, hydrologically intact peatlands is poorly known. Here, field and remote sensing data support model development of peatland extent and thickness for lowland Peruvian Amazonia. We estimate a peatland area of 62,714 (5th and 95th confidence interval percentiles 58,325–67,102 respectively) km<sup>2</sup> and carbon stock of 5.4 (2.6–10.6) Pg C, a value approaching the entire above-ground carbon stock of Peru but contained within just 5% of its land area. Combining the map of peatland extent with national land-cover data we reveal small but growing areas of deforestation and associated CO<sub>2</sub> emissions from peat decomposition, due to conversion to mining, urban areas, and

agriculture. The emissions from peatland areas classified as forest in 2000 represent 1–4% of Peruvian CO<sub>2</sub> forest emissions between 2000 and 2016. We suggest that bespoke monitoring, protection and sustainable management of tropical peatlands are required to avoid further degradation and CO<sub>2</sub> emissions

## **Main text**

While tropical peatlands are known to be among the most carbon-dense ecosystems in the tropics<sup>1,2</sup>, their absolute contribution to the global carbon cycle remains highly uncertain, with recent estimates placing their total below-ground carbon storage between 105 (70–130) and 215 (152–288) Pg C<sup>3,4</sup>. They face various threats including land-use and climate change<sup>4,5</sup>. Deforestation and/or drainage of peatlands inhibit the accumulation of organic matter and promotes rapid decomposition of peat, releasing large quantities of the greenhouse gasses (GHG) CO<sub>2</sub> and N<sub>2</sub>O to the atmosphere<sup>6,7,8,9,10</sup>. Moreover, drained peatlands are prone to fires which lead to large pulses of emissions<sup>11</sup>. The experience of Indonesia provides a cautionary tale: in 1997 alone, it was estimated that between 0.81 and 2.57 Pg C were released as a result of peat and vegetation fires, which at the time equated to 13–40% of global fossil fuel emissions<sup>12</sup>. Indeed, the peatlands of Southeast Asia have already been severely damaged with almost 80% cleared and drained<sup>13</sup>. In contrast, the largest known peatland areas in tropical Africa and South America are thought to remain largely intact<sup>14,15</sup>.

As such, commitments to avoid further deforestation and degradation by 1) promoting conservation and sustainable management of intact peatlands and 2) restoring degraded peatlands, are essential to reducing CO<sub>2</sub> emissions and avoiding global warming of 1.5°C or more<sup>16,17</sup>. A funding mechanism for this is potentially offered by UNFCCC initiatives, including REDD+ and wider National Determined Contributions<sup>18</sup> to the Paris Agreement,

but a necessary first step towards conservation and restoration is reliable mapping of the spatial distribution of peatlands and their carbon stocks, at scales relevant to the development of national policies.

Peru has substantial known regions of hydrologically intact peatland. Previous research identified a large area in the Pastaza-Marañón Foreland Basin in northern Peru (PMFB, Fig. S1), estimating its carbon stock to be 3.14 (0.44–8.15) Pg C including above- and below-ground carbon<sup>2</sup>, and a smaller area in the Madre de Dios (MDD) region of southern Peru holding an estimated 0.03 Pg C<sup>19</sup>). However, published wetland maps<sup>20,21</sup> and visual examination of remote sensing imagery suggest that there are likely other significant peatlands in Peru whose carbon stocks remain unquantified. Even in the best-known region, the PMFB, previous mapping was based on relatively small numbers of peat thickness measurements and did not attempt to model and map the spatial variation in peat thickness<sup>2,22</sup>, one of the greatest sources of uncertainty in the below-ground carbon stock<sup>2</sup>. Rather, the total below-ground carbon stock for the PMFB was estimated by determining the area of different peat-forming vegetation classes (i.e. peatland pole forest, palm swamp and open peatland) and multiplying those areas by a mean below-ground carbon stock for each vegetation class. This approach makes several simplifying assumptions<sup>23</sup>: that these three vegetation classes are always underlain by peat, that peat thickness varies more between than within classes, and that other landcover classes (including some wetland ecosystems such as seasonally flooded forest) never overlie peat<sup>2,22</sup>. In fact, field observations indicate that these assumptions are no longer valid; in particular, peat thickness varies substantially in space, including within single vegetation classes<sup>3,23</sup>. Data-driven maps that more accurately capture the spatial variation in peat thickness and carbon

storage, and that cover not just selected study areas but the whole of Peruvian Amazonia, are required to support national and regional peatland conservation planning.

While Peruvian peatlands are believed to remain largely intact, thus far there has been no quantitative assessment of GHG emissions resulting from landcover change. Moreover, they face varied and increasing threats including agriculture expansion, illegal mining, oil exploration, infrastructure development, and the selective felling of the female *Mauritia flexuosa* palm for commercial purposes<sup>15,23,24,25,26</sup>. In recognition of these threats, legislation has recently been enacted which, for the first time, mandates the explicit protection of peatlands in Peru for climate-change mitigation<sup>27</sup>. Enforcing this legislation effectively will depend on robust mapping of peatland distribution, and on knowledge of the scale and distribution of recent peatland disturbance, none of which is presently available.

Here we present extensive new field observations (Fig. 1) to test whether previous evidence of a relationship between distance to peatland edge and peat thickness found in other tropical peatlands<sup>3</sup>, also applies in Peru. These data are used along with remote sensing imagery to develop the first data-driven models of peatland extent and peat thickness distribution across the whole of lowland Peruvian Amazonia (LPA). We quantify the spatial variation and total peat carbon stock of these peatlands, and associated uncertainties. Finally, we use these models, along with national data on land-cover change, to map peatland disturbance and estimate the associated CO<sub>2</sub> emissions for the period 2000–2016.

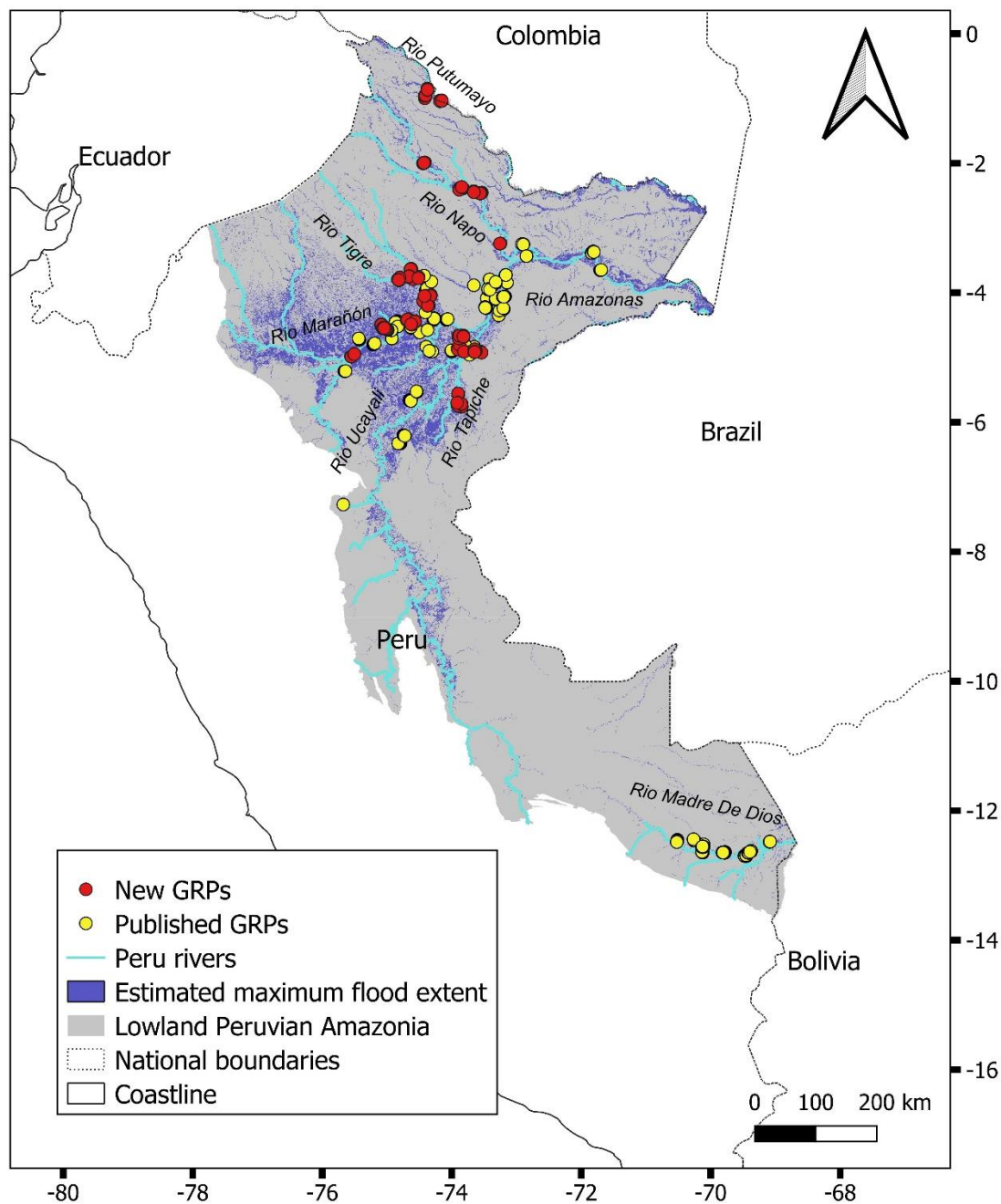


**Figure 1: Distribution of the 1,128 ground reference points (GRPs) sampled for peat thickness and vegetation type data used in this study.** The points include GRPs collected from 2019-2021 as part of this study (red,  $n = 445$ ) as well as published GRPs from<sup>2,19,22,28</sup> (yellow). Estimated maximum flood extent is derived from the wetlands map of ref. <sup>20</sup>. Rivers of Strahler order  $\geq 6$  are shown.

## ***Peat thickness distribution reveals a large carbon store***

We estimate a total peatland extent of 62,714 (58,325–67,102) km<sup>2</sup> (Fig. S2), a mean peat thickness of 203 (179–224) cm (Fig. 2, Fig. S3) and a total below-ground carbon stock of 5.38 (2.55–10.58) Pg C (Fig. S4) across the LPA. In addition to the well-known peatlands of the PMFB and MDD basin, we identify substantial areas of peatland in the Ucayali (11,110 km<sup>2</sup>; 2,258 km in Tapiche sub-basin), Napo (3,670 km<sup>2</sup>) and Putumayo (2,319 km<sup>2</sup>) basins (Fig. 2, Fig. S1, Table S1). Palm swamp is the most extensive peat-forming ecosystem (46,423 km<sup>2</sup>) and therefore contains the greatest stock (3.83 Pg C), despite pole forest and open peatland having higher peat carbon densities (1,054 Mg C ha<sup>-1</sup> and 1,061 Mg C ha<sup>-1</sup> respectively, Table S2). We estimate that 2% of seasonally flooded forest overlies peat, equating to an area of 1,951 km<sup>2</sup> and a peat C stock of 0.11 Pg C (Table S2).

The distribution of peat thickness across the LPA is highly variable, with the greatest mean peat thickness predicted in the Tigre (232 cm), Marañón (230 cm), Tapiche (234 cm), and Napo basins (223 cm) (Fig. 2, Table S1). Our models of peatland area and peat thickness distribution performed well against observations (Table S3, Fig. S5), giving confidence in our results. We ran two separate peat thickness models: one for the MDD basin and another for all the rest of the study area (which contains 97% of total peatland area). The model which excluded the MDD basin performed better ( $p < 0.0001$ ;  $R^2 = 0.66$ , RMSE = 66%, Fig. S5a) than the MDD model ( $p < 0.0001$ ;  $R^2 = 0.38$ , RMSE = 70%, Fig. S5b). We found a significant linear relationship between peat thickness and distance to peatland edge ( $p < 0.0001$ ,  $R^2 = 0.13$ , Fig. S6a). This relationship was more significant when the data from the MDD basin were excluded (giving  $R^2 = 0.39$ ,  $p < 0.0001$ , Fig. S6b) and there was no significant

137 relationship between peat thickness and distance to peatland edge within the MDD data ( $p$   
138  $> 0.1$ ,  $R^2 = 0.005$ , Fig. S6c).

139

140

141

142

143

144

145

146

147

148

149

150

151

152

153

154

155



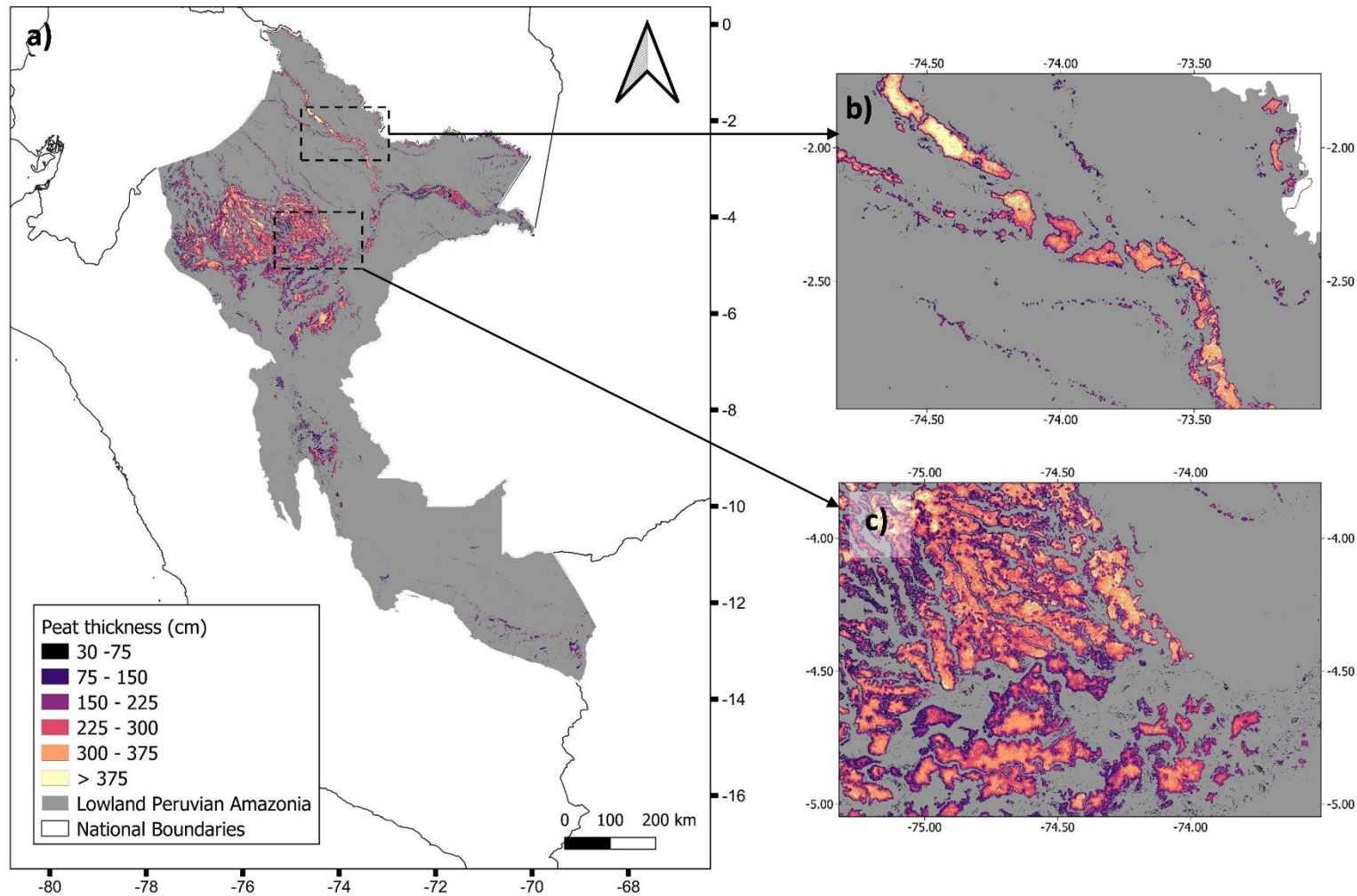


**Figure 2: Distribution of peat thickness.** **a**, predicted distribution of peat thickness across lowland Peruvian Amazonia estimated using random forest regression in Google Earth Engine (median of 1,000 k-folds). **b**, enlargement showing the Napo River. **c**, enlargement showing the Marañón and Tigre rivers. All maps were produced at a resolution of c. 100 m.

## ***CO<sub>2</sub> emissions from land-use change are small but growing***

Our analysis of land-use change data shows that a total peatland area of 1,052 km<sup>2</sup> was drained and/or cleared during 2000–2005, increasing to 1,667 km<sup>2</sup> by 2013–2016 (Table 1). Annual emissions from peat decomposition also increased from 3.26 million Mg CO<sub>2</sub> y<sup>-1</sup> in 2000–2005 to 5.11 million Mg CO<sub>2</sub> y<sup>-1</sup> in 2013–2016, while total estimated emissions accounted for 63.83 million Mg CO<sub>2</sub> during the period 2000–2016 mainly due to deforestation (Fig. 3b1, 3b2). Our analysis suggests rapid increases in CO<sub>2</sub> emissions from conversion to mining, urban areas and agriculture, increasing from 2000 to 2016 by 11 times (from 2,426 to 27,634 Mg CO<sub>2</sub> y<sup>-1</sup>), 9 times (from 2,848 to 26,881 Mg CO<sub>2</sub> y<sup>-1</sup>) and 5 times (from 77,807 to 411,528 Mg CO<sub>2</sub> y<sup>-1</sup>), respectively (see Table S4 and S5 for further detail). These estimates exclude emissions from areas where natural peatland vegetation may have been misclassified in 2000 as secondary forest in the land cover dataset Geobosques (amounting to 1,353 km<sup>2</sup>, Table S5). These misclassified areas were revealed by visual inspection of a Google map image of the department of Loreto by someone with local expert knowledge (Fig. 3a).

For those areas classified as forest in 2000, as accounted for in Peru's 2016 Forest Reference Emission Level report<sup>29</sup>, emissions from peat decomposition represent 0.99–3.72% of total national CO<sub>2</sub> emissions from Lowland Peruvian Amazonian forests (i.e. from peat decomposition and biomass loss due to gross deforestation; Table 1).

**Table 1: Mean CO<sub>2</sub> emissions from peat decomposition (95% CI) and biomass loss across Lowland Peruvian Amazonia (LPA) for four periods between 2000 to 2016 following Geobosques dataset<sup>30</sup>. Peat emissions are from this study, biomass emissions are national estimates <sup>a</sup>.**

	Period			
	2000–2005	2005–2011	2011–2013	2013–2016
Duration (years)	5	6	2	3
Total peatland area with disturbance (km <sup>2</sup> )	1,051.63	1,264.50	1,392.82	1,666.76
Total emissions from peat decomposition due to disturbance (x 10 <sup>6</sup> Mg CO <sub>2</sub> )	16.29 (6.94, 29.16)	23.27 (9.91, 41.61)	8.95 (3.73, 16.03)	15.33 (6.12, 27.59)
Peatland area with disturbance for categories classified as forest in 2000 (km <sup>2</sup> )	158.46	404.38	536.48	808.92
Emissions from peat decomposition due to disturbance for categories classified as forest in 2000 (x 10 <sup>6</sup> Mg CO <sub>2</sub> )	1.25 (0.44, 2.25)	5.33 (1.94, 9.55)	2.98 (1.08, 5.35)	6.40 (2.21, 11.59)
Gross deforestation throughout LPA areas classified as forest in 2000 (km <sup>2</sup> ) <sup>a</sup>	2,483.38	3,945.33	1,915.72	3,303.01
Emissions from biomass loss due to gross deforestation throughout LPA (x 10 <sup>6</sup> Mg CO <sub>2</sub> ) <sup>b</sup>	124.80	198.65	95.85	165.60
% due to peat decomposition for categories classified as forest in 2000	0.99 (0.35, 1.77)	2.61 (0.97, 4.59)	3.02 (1.12, 5.29)	3.72 (1.32, 6.54)

<sup>a</sup> 2016 Forest Reference Emission Level report of Peru<sup>29</sup>.

<sup>b</sup> CO<sub>2</sub> emission from biomass includes both above- and below-ground biomass of living trees as calculated in the 2016 Forest Reference Emission Level report of Peru<sup>29</sup>.

182

183

184

185

186

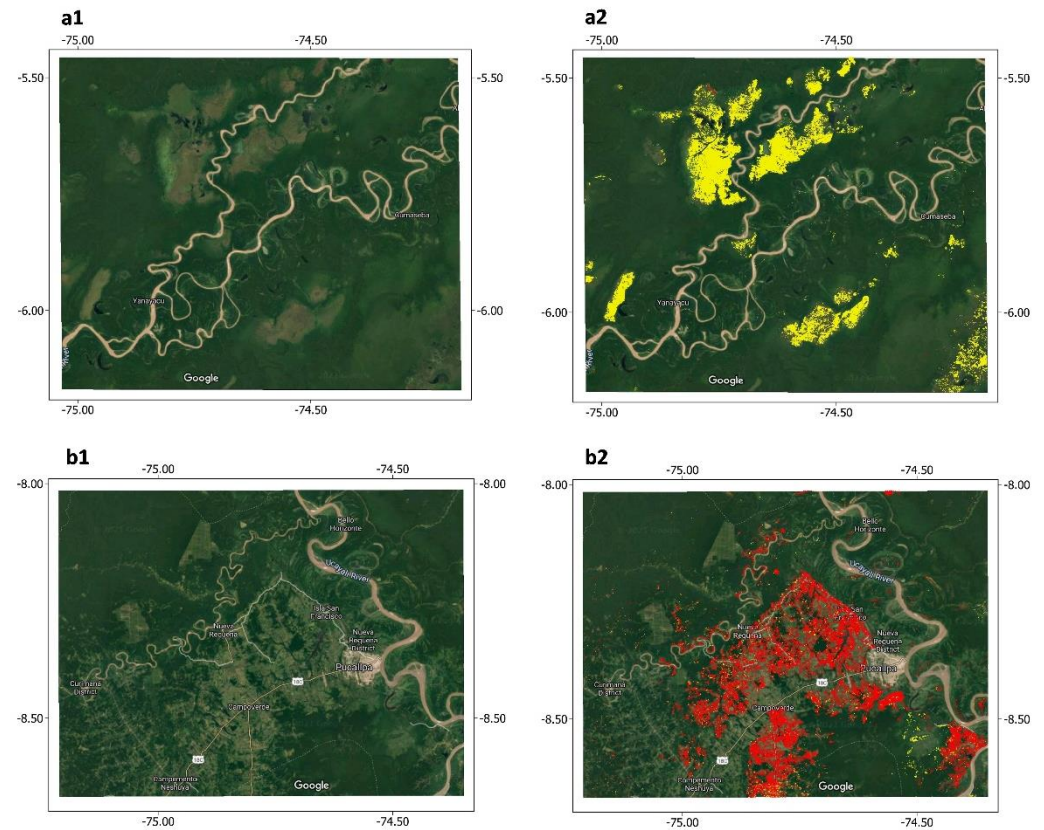
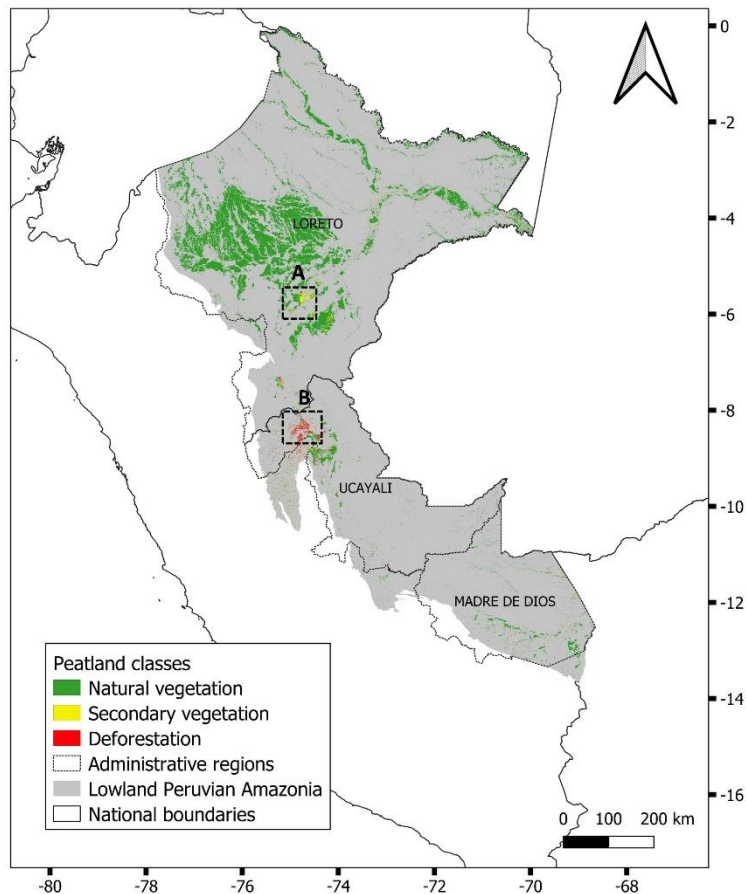


**Figure 3: Distribution of peatlands classified as natural vegetation, secondary vegetation and deforestation based on the 2016 forest land and land use categories within Geobosques<sup>30</sup> in lowland Peruvian Amazonia.** Non-peatland areas are shown in grey, and the relevant departments of Peru are labelled within the study area. Google map images show examples of (A) natural peatland vegetation misclassified as secondary forest (shown in a1, a2) around the Puinahua channel and the Ucayali river in the department of Loreto and (B) peatland areas correctly classified as deforestation (shown in b1, b2) near Pucallpa in the department of Ucayali.

## ***Synthesis and future directions***

Our estimate of the total below-ground carbon stock of 5.38 (2.55–10.58) Pg C across the LPA is 75% of a recent estimate of the entire above-ground C stock of Peru<sup>31</sup>, and approximately doubles previous estimates of the Peruvian tropical peat stock calculated for the PMFB and the MDD regions only<sup>2,19,22</sup>. Our maps are driven by intensive field sampling which has, for the first time, generated peat thickness data widely across LPA, and which confirms that significant peatlands extend far beyond the relatively well-studied PMFB. Across the main peat-forming landcover classes of pole forest, open peatland and palm swamp, above-ground carbon densities (Table S2,<sup>23</sup>) are an order of magnitude lower than respective peat carbon densities, totalling 0.45 Pg C (Table S2). Summing the above- and below-ground carbon stocks gives a central estimate of 5.83 Pg C stored in LPA peatlands. The quantitative uncertainties around the peatland carbon stock are reduced compared to previous studies despite our study covering an area > 5 times greater<sup>2,22</sup>. Future improvement may be gained by collecting field data where they are still lacking, notably the northwest PMFB and parts of the Ucayali (e.g. around Pucallpa) and Morona basins. Unlike previous studies<sup>2,22</sup> our study placed no constraints on which landcover classes peat can form under, and we predict that around 2% of seasonally flooded forest is underlain by peat. This suggests that the search for peat should not be solely limited to the well-known peat-forming vegetation types of palm swamp, pole forest and open peatland. In addition to landcover classification maps, we recommend that future fieldwork is informed by examining maps and remote sensing imagery related to hydrology and inundation, such as height above nearest drainage (HAND)<sup>32</sup>, normalized difference water index (NDWI)<sup>33</sup> and ALOS-PALSAR<sup>34</sup> (where possible multi-temporal images).

Our approach is driven by remote sensing layers with global coverage and can thus be readily adapted to other regions, provided sufficient field data are available for calibration and validation. Our results call for caution in treating all tropical peatlands as similar, and demonstrate the importance of field data. For example, distance to peatland edge has been found to correlate with peat thickness in other regions such as the Congo basin<sup>3</sup>, and in most of the basins we studied in Peru. However, we found no significant linear relationship between peat thickness and distance to peatland edge for the data in the MDD basin ( $p > 0.1$ ,  $R^2 = 0.005$ , Fig. S6c). Householder et al.<sup>19</sup> suggest that this may be because of specific geological conditions in this region: many of the deepest peats in the MDD are often located adjacent to upland (*terra firme*) terraces, close to the peatland edge. This means that the relationship between peat thickness and distance to peatland edge is more complex in MDD than in other regions. Past research points to geomorphological differences between northern and southern parts of Peruvian Amazonia<sup>35</sup>: while floodplains in northern Amazonia are often wide, rivers in southern Amazonia more often have narrow floodplains confined by terraces. We recommend that new transects should aim to target a range of landscape types (e.g. based on elevation maps) and where possible should cover the full cross-section of each individual peatland. In spite of this limitation, our random forest regression model for the MDD region performs reasonably well.

This study assesses CO<sub>2</sub> emissions resulting from peat decomposition due to land-cover change in Peru. Our results suggest that land cover change in the peatlands of the LPA has thus far been restricted to a few hotspot areas, with the largest area of deforestation identified near Pucallpa in the department of Ucayali, an area where recent ground observations confirm the presence of deforested peatlands (<sup>26</sup>; E. Honorio, pers. comm.). Access to these peatlands has been facilitated by the development of roads and the

increasing demand for land for commercial plantations (e.g. oil palm and rice<sup>36,37</sup>, D. Garcia-Soria, pers. comm.). Overall, the estimated emissions from peat decomposition remain low in Peru but our analysis suggests that the annual emissions are increasing. These findings have two implications for the conservation of these ecosystems. Firstly, the low current emissions support the view that the extensive peatland complex of the LPA is an emblematic example of hydrologically intact moist tropical forest with high structural integrity and therefore should be a high conservation priority<sup>23,38,39</sup>. Investment is required to promote protection and sustainable management of these widespread and extremely carbon-dense ecosystems, before emissions rise over the coming decades<sup>40,41</sup>. Secondly, the increasing threats and rising emissions from specific land-use transitions in some peatlands mean that it is important to improve detection of deforestation and secondary vegetation across the full range of peatland forest types, and to make more extensive measurements of greenhouse gas emissions associated with specific land-use transitions across the different forest types<sup>7,8,9</sup>.

Taken together, our results indicate a carbon stock within the peatlands of LPA which is three-quarters as large as the entire above-ground carbon stock of Peru<sup>31</sup> but contained within just 5% of its land area. The peatlands also contribute substantial ecosystem and floristic diversity to the Amazon<sup>42,43</sup>. While our study indicates that these peatlands remain largely intact, they face varied and growing threats<sup>15,37</sup>. Our mapping and carbon stock estimates may be used to support the implementation and enforcement of recent legislation aimed at reducing emissions<sup>27</sup> and should act to encourage national and international investment in monitoring, protection and sustainable management of Peru's peatlands, in order that they avoid a similar fate to the heavily degraded peatlands of Southeast Asia<sup>37</sup>.

## **Corresponding author**

Correspondence to Adam Hastie.

## **Acknowledgments**

This work was funded by NERC (Grant ref. NE/R000751/1)- I.T.L, A.H, K.H.R, E.T.A.M, C.M.A, T.R.B, G.D, E.C.D.G; Leverhulme Trust (Grant ref. RPG-2018-306)-K.H.R, L.E.S.C, C.E.W; Gordon and Betty Moore Foundation (Grant #5439, MonANPeru network)-T.R.B, E.N.H.C, G.F; Wildlife Conservation Society-E.N.H.C; Concytec/British Council/Embajada Británica Lima/Newton Fund (Grant ref. 220-2018)-E.N.H.C, J.D; Concytec/NERC/Embajada Británica Lima/Newton Fund (Grant ref. 001-2019)-E.N.H.C, N.D; the governments of the United States of America (Grant No. MTO-069018) & Norway (Grant Agreement No. QZA-12/0882)-K.H; and NERC Knowledge Exchange Fellowship (Grant Ref No. NE/V018760/1)-E.N.H.C. We thank SERNANP, SERFOR and GERFOR for providing research permits, and the different indigenous and local communities, research stations and tourist companies for giving consent and allowing access to the forests. We acknowledge the invaluable support of technicians Julio Irarica, Julio Sanchez, Hugo Vásquez and Rider Flores, without whom much of the field work would not have been possible. We would like to thank the reviewers for the time and effort they took to carefully review the paper. For the purpose of open access, the author has applied a 'Creative Commons Attribution (CC BY) licence to any Author Accepted Manuscript version arising.

## **Author Contributions**

A.H, I.T.L, E.N.H.C, E.T.A.M, K.H.R, T.R.B, L.E.S.C and C.E.W all contributed to the conception, development and design of the study. A.H and E.N.H.C performed the analysis with input



from E.T.A.M, K.H, I.T.L, L.E.S.C and P.R-V. A.H and E.N.H.C wrote the manuscript with input from all co-authors. New field data was collected by J.R, A.H, C.M.A, I.T.L, L.E.S.C, C.E.W, N.D, C.J.C-O, G.D, J.D.A, G.F, D.R, and J.G. E.H, O.L, F.D, J.P.J and M.T provided data.

## Competing Interests

The authors declare no competing interests

## References

1. Dommain, R., Couwenberg, J. & Joosten, H. Development and carbon sequestration of tropical peat domes in south-east Asia: links to post-glacial sea-level changes and Holocene climate variability. *Quat. Sci. Rev.* **30**, 999–1010 (2011).
2. Draper, F. C. *et al.* The distribution and amount of carbon in the largest peatland complex in Amazonia. *Environ. Res. Lett.* **9**, 124017 (2014).
3. Dargie, G. C. *et al.* Age, extent and carbon storage of the central Congo Basin peatland complex. *Nature* **542**, 86 (2017).
4. Ribeiro, K. *et al.* Tropical peatlands and their contribution to the global carbon cycle and climate change. *Glob. Chang. Biol.* **27**, 489–505 (2021).
5. Wang, S., Zhuang, Q., Lähteenoja, O., Draper, F. C. & Cadillo-Quiroz, H. Potential shift from a carbon sink to a source in Amazonian peatlands under a changing climate. *Proc. Natl. Acad. Sci.* **115**, 12407–12412 (2018).
6. IPCC. *2013 Supplement to the 2006 IPCC Guidelines for National Greenhouse Gas Inventories: Wetlands. Prepared by Hiraishi, T., Krug, T., Tanabe, K., Srivastava, N.,*

- 308        *Baasansuren, J., Fukuda, M. and Troxler, T.G. (eds). (2014).*
- 309        7.     van Lent, J., Hergoualc'h, K., Verchot, L., Oenema, O. & van Groenigen, J. W.
- 310        Greenhouse gas emissions along a peat swamp forest degradation gradient in the
- 311        Peruvian Amazon: soil moisture and palm roots effects. *Mitig. Adapt. Strateg. Glob.*
- 312        *Chang.* **24**, 625–643 (2019).
- 313        8.     van Lent, J. Land-use change and greenhouse gas emissions in the tropics: Forest
- 314        degradation on peat soils. PhD dissertation, Wageningen University. (2020).
- 315        9.     Hergoualc'h, K. *et al.* Spatial and temporal variability of soil N<sub>2</sub>O and CH<sub>4</sub> fluxes along
- 316        a degradation gradient in a palm swamp peat forest in the Peruvian Amazon. *Glob.*
- 317        *Chang. Biol.* **26**, 7198–7216 (2020).
- 318        10.    Swails, E., Hergoualc'h, K., Verchot, L., Novita, N. & Lawrence, D. Spatio-Temporal
- 319        Variability of Peat CH<sub>4</sub> and N<sub>2</sub>O Fluxes and Their Contribution to Peat GHG Budgets in
- 320        Indonesian Forests and Oil Palm Plantations. *Front. Environ. Sci.* **9**, 48 (2021).
- 321        11.    Gaveau, D. L. A. *et al.* Major atmospheric emissions from peat fires in Southeast Asia
- 322        during non-drought years: evidence from the 2013 Sumatran fires. *Sci. Rep.* **4**, 6112
- 323        (2014).
- 324        12.    Page, S. E. *et al.* The amount of carbon released from peat and forest fires in
- 325        Indonesia during 1997. *Nature* **420**, 61–65 (2002).
- 326        13.    Mishra, S. *et al.* Degradation of Southeast Asian tropical peatlands and integrated
- 327        strategies for their better management and restoration. *J. Appl. Ecol.* **58**, 1370–1387
- 328        (2021).
- 329        14.    Dargie, G. C. *et al.* Congo Basin peatlands: threats and conservation priorities. *Mitig.*

- 330        *Adapt. Strateg. Glob. Chang.* **24**, 669–686 (2019).
- 331    15.    Roucoux, K. H. *et al.* Threats to intact tropical peatlands and opportunities for their  
332        conservation. *Conserv. Biol.* **31**, 1283–1292 (2017).
- 333    16.    Griscom, B. W. *et al.* Natural climate solutions. *Proc. Natl. Acad. Sci.* **114**, 11645–  
334        11650 (2017).
- 335    17.    Girardin, C.A.J., Jenkins, S., Seddon, N., Allen, M., Lewis, S.L., Wheeler, C.E., Griscom,  
336        B.W. & Malhi, Y. . Nature-based solutions can help cool the planet — if we act now.  
337        *Nature* **593**, 191–194 (2021).
- 338    18.    Murdiyarso, D., Lilleskov, E. & Kolka, R. Tropical peatlands under siege: the need for  
339        evidence-based policies and strategies. *Mitig. Adapt. Strateg. Glob. Chang.* **24**, 493–  
340        505 (2019).
- 341    19.    Householder, J. E., Janovec, J. P., Tobler, M. W., Page, S. & Lähteenoja, O. Peatlands  
342        of the Madre de Dios River of Peru: Distribution, Geomorphology, and Habitat  
343        Diversity. *Wetlands* **32**, 359–368 (2012).
- 344    20.    Hess, L. L. *et al.* Wetlands of the Lowland Amazon Basin: Extent, Vegetative Cover,  
345        and Dual-season Inundated Area as Mapped with JERS-1 Synthetic Aperture Radar.  
346        *Wetlands* **35**, 745–756 (2015).
- 347    21.    Gumbricht, T. *et al.* An expert system model for mapping tropical wetlands and  
348        peatlands reveals South America as the largest contributor. *Glob. Chang. Biol.* **23**,  
349        3581–3599 (2017).
- 350    22.    Lähteenoja, O. *et al.* The large Amazonian peatland carbon sink in the subsiding  
351        Pastaza-Marañón foreland basin, Peru. *Glob. Chang. Biol.* **18**, 164–178 (2012).

- 352 23. Coronado, E. N. H. *et al.* Intensive field sampling increases the known extent of  
353 carbon-rich Amazonian peatland pole forests. *Environ. Res. Lett.* **16**, 74048 (2021).
- 354 24. Hergoualc'h, K., Gutiérrez-Vélez, V. H., Menton, M. & Verchot, L. V. Characterizing  
355 degradation of palm swamp peatlands from space and on the ground: An exploratory  
356 study in the Peruvian Amazon. *For. Ecol. Manage.* **393**, 63–73 (2017).
- 357 25. Baker, T.R., del Castillo Torres, D., Honorio Coronado, E., Lawson, I., Brañas, M.M.,  
358 Montoya, M., Roucoux, K. The challenges for achieving conservation and sustainable  
359 development within the wetlands of the Pastaza Marañón basin, Peru. pp. 155-175 in  
360 '*Peru: Deforestation in times of climate change*' (ed. A. Chirif), *International Work*  
361 *Group for Indigenous Affairs*,. (2019).
- 362 26. López Gonzales, M.; Hergoualc'h, K.; Angulo Núñez, Ó.; Baker, T.; Chimner, R.; del  
363 Águila Pasquel, J.; del Castillo Torres, D.; Freitas Alvarado, L.; Fuentealba Durand, B.;  
364 García Gonzales, E.; Honorio Coronado, E.; Kazuyo, H.; Lilleskov, E.; Málaga Durán, F.  
365 What do we know about Peruvian peatlands? Bogor, Indonesia. Retrieved from  
366 [https://www.cifor.org/publications/pdf\\_files/OccPapers/OP-210.pdf](https://www.cifor.org/publications/pdf_files/OccPapers/OP-210.pdf) (2020).
- 367 27. MINAM. Decreto Supremo N° 006-2021-MINAM (2021).
- 368 28. Lähteenoja, O., Ruokolainen, K., Schulman, L. & Oinonen, M. Amazonian peatlands:  
369 an ignored C sink and potential source. *Glob. Chang. Biol.* **15**, 2311–2320 (2009).
- 370 29. MINAM. Peru's submission of a Forest Reference Emission Level (FREL) for reducing  
371 emissions from deforestation in the Peruvian Amazon. 77 pages (2016).
- 372 30. MINAM. *Coberturas de uso y cambio de uso de la tierra para los periodos 2000-2005,*  
373 *2005-2011, 2011-2013, 2013-2016. Monitoreo de los cambios sobre la cobertura de*

374        *los bosques peruanos – Geobosques*. (2020).

375    31.    Csillik, O., Kumar, P., Mascaro, J., O’Shea, T. & Asner, G. P. Monitoring tropical forest  
376        carbon stocks and emissions using Planet satellite data. *Sci. Rep.* **9**, 17831 (2019).

377    32.    Donchyts, Gennadii., Winsemius, Hessel., Schellekens, Jaap., Erickson, Tyler., Gao,  
378        Hongkai., Savenije, Hubert., and van de Giesen, N. ‘Global 30m Height Above the  
379        Nearest Drainage (HAND)’ in (Geophysical Research Abstracts, Vol. 18, EGU2016-  
380        17445-3, 2016, EGU General Assembly, 2016).

381    33.    Drusch, M. *et al.* Sentinel-2: ESA’s Optical High-Resolution Mission for GMES  
382        Operational Services. *Remote Sens. Environ.* **120**, 25–36 (2012).

383    34.    Shimada, M. *et al.* New global forest/non-forest maps from ALOS PALSAR data (2007–  
384        2010). *Remote Sens. Environ.* **155**, 13–31 (2014).

385    35.    Toivonen, T., Mäki, S. & Kalliola, R. The riverscape of Western Amazonia – a  
386        quantitative approach to the fluvial biogeography of the region. *J. Biogeogr.* **34**,  
387        1374–1387 (2007).

388    36.    Vijay, V., Reid, C. D., Finer, M., Jenkins, C. N. & Pimm, S. L. Deforestation risks posed  
389        by oil palm expansion in the Peruvian Amazon. *Environ. Res. Lett.* **13**, 114010 (2018).

390    37.    Lilleskov, E. *et al.* Is Indonesian peatland loss a cautionary tale for Peru? A two-  
391        country comparison of the magnitude and causes of tropical peatland degradation.  
392        *Mitig. Adapt. Strateg. Glob. Chang.* **24**, 591–623 (2019).

393    38.    Watson, J. E. M. *et al.* The exceptional value of intact forest ecosystems. *Nat. Ecol.*  
394        *Evol.* **2**, 599–610 (2018).

39. Hansen, A. J. *et al.* A policy-driven framework for conserving the best of Earth's remaining moist tropical forests. *Nat. Ecol. Evol.* **4**, 1377–1384 (2020).
40. Maxwell, S. L. *et al.* Degradation and forgone removals increase the carbon impact of intact forest loss by 626%. *Sci. Adv.* **5**, 10 (2019).
41. Grantham, H. S. *et al.* Anthropogenic modification of forests means only 40% of remaining forests have high ecosystem integrity. *Nat. Commun.* **11**, 5978 (2020).
42. Lähteenoja, O. & Page, S. High diversity of tropical peatland ecosystem types in the Pastaza-Marañón basin, Peruvian Amazonia. *J. Geophys. Res. Biogeosciences* **116**, (2011).
43. Draper, F. C. *et al.* Peatland forests are the least diverse tree communities documented in Amazonia, but contribute to high regional beta-diversity. *Ecography*, **41**, 1256–1269 (2018).

## Methods

### *Fieldwork*

Between 2019 and 2021, we collected 445 new ground reference points (GRPs) within LPA (Fig. 1, 294 of which were presented by ref.<sup>23</sup>) collecting data on the substrate (i.e. peat thickness, where peat is present) and vegetation type (e.g. palm swamp). We focused data collection on regions with no existing GRPs, where peat was believed to be present based on remote sensing imagery (e.g. various Landsat 8 [Fig. S7] and Sentinel 2 bands), including

the Napo, Putumayo, Tapiche and Tigre river basins (Fig. 1, Fig. S1), using the only available means of access, i.e. via rivers and streams. We also collected new data on peat thickness and carbon concentration from under-sampled peatland ecosystems (e.g. peatland pole forest). We made the sampling as spatially representative as possible within the constraints of logistical feasibility, personal safety and accessibility, which are substantial in these remote regions of Peru. The previously published datasets which we incorporated here were also subject to the same constraints.

Where present, peat thickness was measured with an auger or Russian-type peat corer, either along transects perpendicular to the river at intervals of 200–500 m, or at the four corners and centre of the vegetation plots (see below) in which case the value for peat thickness used is the mean of five point measurements. Working along transects leading away from the river and into the peatlands allowed us to sample across wide hydrological and topographic gradients, including both minerotrophic and ombrotrophic ecosystems. At 91 of these GRPs, we conducted 1 ha, 0.5 ha or 0.1 ha vegetation plot surveys (collecting floristic data) for quantitative classification of ecosystem type<sup>23,43</sup>. Additionally, we used 218 previously published GRPs<sup>2,22,28</sup> (24 with floristic data) collected using a similar transect-based sampling strategy in northern Peru and 465 GRPs<sup>19</sup> (148 with floristic data) collected in southern Peru, amounting to a total of 1,128 GRPs (Fig. 1). Of these, 887 GRPs (Fig. S8) indicated the presence of peat (defined as an organic layer  $\geq 30$  cm thick<sup>44</sup>). Two examples of peat thickness measurement transects in the Napo basin are shown in Figure S7.

The majority of peat thickness observations do not have corresponding carbon concentration measurements and thus we cannot enforce a precise cut-off in terms of carbon content. However, we visually identified peat and underlying sediments in the field

on the basis of their physical properties (e.g. colour, structure, texture) and composition (e.g. wood, roots, mineral components)<sup>45,46</sup>. At 35 vegetation plots identified by fieldworkers as being on peat, we took sediment samples in the near-basal peat, transition zone and underlying mineral sediment (typically silts or clays) and measured loss on ignition (LOI) in each to test the visual assessments. The peat, transition zone and mineral samples had mean LOI values of 70%, 28% and 13% respectively (see Table S6). This gives us confidence that fieldworkers in this region are able to visually identify peat (in this case, soil with an LOI of at least 50%), as there is typically a clear and distinct transition to mineral sediment in Peruvian peatlands.

#### ***Map of predicted peatland extent in lowland Peruvian Amazonia***

We created a 50 m resolution map (Fig. S2) of predicted peatland extent in LPA (defined here as the area covered by two of the ecozones recognized by Peru's Ministry of Environment: Ecozone Selva Baja and Ecozone Hidromórfica<sup>47</sup>). Firstly, we ran a supervised random forest (RF) algorithm (200 trees) in Google Earth Engine to predict the distribution of five classes: peat below forest (PBF), peat below non-forest (i.e. herbaceous vegetation and shrubland, PBNF), non-peat below forest (NBF), non-peat below non-forest (NBN) and open water (WA). The model was trained and validated (50/50 split of polygons) using peat thickness measurements and information on the overlying vegetation, and driven using a stack of seven remote sensing layers including two Sentinel-2 indices (NDVI & NDWI<sup>33</sup>), three ALOS PALSAR-2 bands (HH, HV, HH/HV<sup>34</sup>), SRTM 30 m digital elevation<sup>48</sup> (Table S7), and an extended version of a landcover classification produced previously<sup>23</sup> (Fig. S9; Supplementary Information has further details). The PBF and PBNF categories were amalgamated to form the map of total peatland extent in Fig. S2. We calculated 5<sup>th</sup> and 95<sup>th</sup>



confidence interval percentiles for peatland area using the area and accuracy of each class, applying the method described in ref. <sup>49</sup> (equations 9–13), following ref. <sup>2</sup> and recommended by the Global Forest Observations Initiative.

#### ***Model of peat thickness distribution***

Testing showed that peat thickness increases with distance to peatland edge ( $R^2 = 0.13$ ,  $p < 0.0001$ , Fig. S6), indicating that the deepest peat is typically found in the centre of a peatland. We thus calculated distance to peatland edge for each model grid, using our map of peatland extent. We used the 1,128 peat thickness measurements as training data, supplemented with points that we assumed to lack peat located along known rivers and urban areas (based on a combination of local knowledge and inspection of Sentinel-2 and Landsat 8 images), amounting to a final dataset of 1,359 points. The model was run at 100 m resolution in Google Earth Engine and driven by the stack of remote sensing layers, with two additional layers: distance to peatland edge, and height above nearest drainage (HAND<sup>32</sup>) (Table S8).

In order to robustly test model performance, we performed a series of validations which accounted for spatial autocorrelation. Training the model using data only from within the PMFB ( $n = 717$ ) and testing against data from outside the PMFB in Northern Peru (Napo, Putumayo and upper Amazon basins,  $n = 155$ ), the model performed relatively well (Observed vs Predicted peat thickness,  $p < 0.0001$ ;  $R^2 = 0.56$ , Fig. S10a). However, the same model (trained using only PMFB data) was unable to predict variation in peat thickness observed in the Madre De Dios (MDD) basin data ( $n = 478$ ,  $p > 0.50$ ;  $R^2 = 0.00$ , Fig. S10b). For this reason, we decided to run two separate models for the final analysis, one using data only within the MDD basin ( $n = 477$ , no. model trees = 100), and another using all other data

points ( $n = 867$ , no. model trees = 50). Model performance was lower in the model which used only MDD data ( $p < 0.0001$ ;  $R^2 = 0.38$ , RMSE = 70%, Fig. S5b) than that using all other data points (Observed Vs Predicted peat thickness,  $p < 0.0001$ ;  $R^2 = 0.66$ , RMSE = 66%, Fig. S5a). We independently validated both models by training each with 80% of the data (randomly selected) and testing with the remaining 20% (Fig. S5c, d).

To account for the uncertainty associated with our estimate of peat thickness distribution, we ran a k-fold analysis as in<sup>50</sup>, splitting the data into 1,000 folds, and therefore generating 1,000 predictions of peat thickness per pixel. We took the median, 5th and 95th percentiles of the 1,000 predictions to represent our best estimate (Fig. 2a), minimum (Fig. S3a) and maximum (Fig. S3b) peat thickness distributions. We subsequently masked the maps of peat thickness distribution using the map of peatland extent (Fig. S2), thus restricting our model to only regions predicted to contain peat.

### ***Below-ground carbon stock***

A dataset of 68 stratigraphic profiles of carbon concentration (%) and dry bulk density (DBD,  $\text{g cm}^{-3}$ ) was compiled using data from refs<sup>2,22,23,28,51</sup> (see Table S9). This includes ten new peat profiles collected as part of this study and described in<sup>23</sup> (see Table S4 of Honorio Coronado et al., 2021<sup>23</sup>). We calculated peat carbon stock (PC,  $\text{Mg C ha}^{-1}$ ) from the peat cores by multiplying peat thickness (cm) by DBD and carbon concentration evaluated at regular intervals down the peat profile to the base of the peat. Laboratory conditions varied depending on the study and can be found in the original papers, along with information on protocols. The studies used a variety of standard methodologies to determine sample carbon concentrations. In line with our definition of peat, we only retained cores in which

the peat was  $\geq 30$  cm thick, with a mean LOI of  $\geq 50\%$ , and those collected using a Russian corer to ensure that DBD measurements were based on a reliable volumetric sample.

We performed a sensitivity analysis to test which of the three components of PC (i.e. peat thickness, DBD and carbon concentration) was most important. Peat thickness was found to be the most important determinant of total PC ( $p < 0.0001$ ;  $R^2 = 0.81$ , Fig. S11). We thus used our model of peat thickness distribution to estimate total PC for each 100 m grid-cell and then summed across the entire LPA to produce a total value for the peat carbon stock.

In order to produce uncertainty bounds for our estimate of the total peat C stock, we ran a Monte Carlo analysis which accounted for the uncertainty in each stage of our methodology. We ran 1,000 simulations for PC, constrained using the standard error of the b-estimates from the regression equation (peat thickness vs PC, Fig. S11). This was performed twice, once using the 5<sup>th</sup> and then the 95<sup>th</sup> percentile distribution of peat thickness calculated previously (Fig. S3). These 1,000 PC simulations were in turn multiplied by 1,000 simulations of peatland area per grid, constrained by the confidence intervals calculated previously. Finally, the maps of the 5<sup>th</sup> and 95<sup>th</sup> percentile of peat C stock per grid were summed across LPA to derive the final minimum and maximum uncertainty bounds.

#### ***Activity data and emissions from peat decomposition***

To estimate changes in forest cover, we used reports of activity data provided by Peru's national monitoring platform, Geobosques<sup>30</sup>. These reports were generated using Landsat 7 and 8 images from 2001 to 2016 at 30 m resolution, with cumulative areas of different land uses for the year 2000<sup>30</sup>. In these data, Peruvian Amazonia is classified into 11 land uses for the periods 2000–2005, 2005–2011, 2011–2013, and 2013–2016. Figure 3 shows our

predicted peatland map (produced by re-running our model at 30 m resolution to match the activity dataset) grouping the categories that represent natural vegetation (forest, forest on wetland, wet savannah, water body, non-forest on wetland), secondary vegetation, and deforested areas (agriculture, pasture, urban areas, mining areas, bare ground).

Emission factors for organic soils were taken from Chapter 2 of the 2013 Supplement to the 2006 IPCC Guidelines for the National GHG Inventory for Wetlands<sup>6</sup>. The values range from 7.5 Mg C ha<sup>-1</sup> y<sup>-1</sup> for secondary vegetation to 9.6 Mg C ha<sup>-1</sup> y<sup>-1</sup> for deforested peatlands (Table S4). These IPCC values are intended to be used for drained peatlands, but peatland disturbance in Peru does not necessarily entail drainage. Nonetheless, undrained secondary forests on peat in Indonesia lose soil carbon (1.4 Mg C ha<sup>-1</sup> y<sup>-1</sup>; <sup>10</sup>) at a similar rate to shallow-drained plantations (1.5 Mg C ha<sup>-1</sup> y<sup>-1</sup>; <sup>6</sup>), and CO<sub>2</sub> emissions in highly degraded undrained peatlands in Peru (e.g. degraded *Mauritia*-dominated palm swamps classified as secondary vegetation: 7.1 Mg C ha<sup>-1</sup> y<sup>-1</sup>; <sup>8</sup>) fall within the range of the values of deforested drained peatlands in Indonesia (1.5–14.0 Mg C ha<sup>-1</sup> y<sup>-1</sup>; <sup>6</sup>, Table S5). Therefore, we assume the IPCC emission factors are acceptable estimates for drained or undrained peatlands in Peru, which is reasonable given that it matches the available evidence.

Total CO<sub>2</sub> emissions following land use change due to inferred peat decomposition were estimated following the equation 2.3 from Chapter 2 in the IPCC Wetlands Supplement<sup>6</sup>:

$$PDE = \sum_{ij=0}^n A_{ij} * EF_{ij} * t * 44/12 \quad (1)$$

Where  $PDE$  is total CO<sub>2</sub> emissions from peat decomposition (Mg CO<sub>2</sub>);  $A$  is the area (ha) on peatlands of the original land-use category- $i$  that was converted into category- $j$  during the time period  $t$  (years);  $EF$  is the mean annual emission factor of peat decomposition assigned to the conversion from category- $i$  to category- $j$  (Mg C ha<sup>-1</sup> y<sup>-1</sup>) and converted to CO<sub>2</sub> by multiplying by the atomic mass factor of 44/12<sup>52,53</sup>. For example, within peatlands (according to our map), forest on wetland (ecosystem saturated with water and assumed zero CO<sub>2</sub> emissions) that is converted to mining area (ecosystem assumed similar to drained grasslands with emissions of 9.6 Mg C ha<sup>-1</sup> y<sup>-1</sup>) will receive an  $EF$  value of 4.8 Mg C ha<sup>-1</sup> y<sup>-1</sup> following<sup>52</sup> (Table S5).

## Data availability

An interactive map of modelled peatland extent (50 m resolution) can be viewed here:

<https://code.earthengine.google.com/a07b25e62adbe714afa77e4a3e423b1b>

and source map downloaded here:

An interactive map of modelled landcover class (50 m resolution) can be viewed here:

<https://code.earthengine.google.com/f3a655bbf36db6121be1d7fd09991530>

and source map downloaded here: <https://datashare.ed.ac.uk/handle/10283/4364>

An interactive map of modelled peat thickness distribution (100 m resolution) can be

viewed here: <https://code.earthengine.google.com/8845760a7e086df8b1e66075985ea705>

and source maps downloaded here: <https://datashare.ed.ac.uk/handle/10283/4364>

An interactive map of modelled peat carbon (100 m resolution) can be viewed here:

<https://code.earthengine.google.com/394ed8b119c1913f7c5f5b6a969ec19f>

and source maps downloaded here: <https://datashare.ed.ac.uk/handle/10283/4364>

The MINAM Geobosques<sup>30</sup> raster file can be downloaded here:

<https://geobosques.minam.gob.pe/geobosque/view/descargas.php?122345gx345w34gg>

## Code availability

The above Google Earth Engine links include code for some basic analysis of the maps. Code for other parts of the analysis will be made available upon reasonable request to the corresponding author.

#### **Additional references for methods**

44. Page, S. E., Rieley, J. O. & Banks, C. J. Global and regional importance of the tropical peatland carbon pool. *Glob. Chang. Biol.* **17**, 798–818 (2011).
45. Troels-Smith, J. Characterisation of unconsolidated sediments. *Danmarks Geol. Undersogelse IV*, 73 (1955).
46. Kershaw., A. . A modification of the Troels-Smith system of sediment description and portrayal. *Quat. Australas.* **15**, 63–68 (1997).
47. Málaga, N., Giudice, R., Vargas, C., y Rojas, E. *Estimación de los contenidos de carbono de la biomasa aérea en los bosques de Perú. Lima: Ministerio del Ambiente del Perú.* (2014).
48. Farr, T. G. *et al.* The Shuttle Radar Topography Mission. *Rev. Geophys.* **45**, (2007).
49. Olofsson, P., Foody, G. M., Stehman, S. V & Woodcock, C. E. Making better use of accuracy data in land change studies: Estimating accuracy and area and quantifying uncertainty using stratified estimation. *Remote Sens. Environ.* **129**, 122–131 (2013).
50. Rodríguez-Veiga, P. *et al.* Carbon Stocks and Fluxes in Kenyan Forests and Wooded Grasslands Derived from Earth Observation and Model-Data Fusion. *Remote Sensing* vol. 12 (2020).
51. Bhomia, R. K. *et al.* Impacts of *Mauritia flexuosa* degradation on the carbon stocks of

602 freshwater peatlands in the Pastaza-Marañón river basin of the Peruvian Amazon.  
603 *Mitig. Adapt. Strateg. Glob. Chang.* **24**, 645–668 (2019).

604 52. Ministry of Environment and Forestry. Indonesia. *MoEF, 2016, National Forest*  
605 *Reference Emission Level for Deforestation and Forest Degradation: In the Context of*  
606 *Decision 1/CP.16 para 70 UNFCCC (Encourages developing country Parties to*  
607 *contribute to mitigation actions in the forest sector), Directorate . (2016).*

608 53. IPCC. *IPCC guidelines for National Greenhouse Gas Inventories. Agriculture, forestry*  
609 *and other land use (AFOLU), Vol. 4, Eggleston, S., L. Buendia, K. Miwa, T. Ngara, and*  
610 *K. Tanabe (eds.). Prepared by the National Greenhouse Gas Inventories Programme,*  
611 *Institu.* <https://www.ipcc-nggip.iges.or.jp/public/2006gl/vol4> (2006).  
612